Al-Mustansiriyah Journal of Science
ISSN: 1814-635X (print), ISSN:2521-3520 (online)
Volume 30, Issue 4, 2019
DOI: http://doi.org/10.23851/mjs.v30i4.699

Research Article Open Access

Magnetic Properties of the Spinel Ferrite $MgZnFe_2O_4$ Deposited on Glass Using Pulsed-Laser Ablation Method

Taha H. Lazem[1], Kadhim J. Kadhim[1], Atheer I. A.[2]
[1]Department of physics, College of science, Mustansiriyah University, IRAQ
[2]Shool of Applied Sciences, University of Technology, IRAQ
*Correspondent author email: tahalazem78@yahoo.com

Article Info

Received
15/07/2019

Accepted
23/09/2019

Published
15/01/2020

Abstract

Sol-gel deposition of spinel ferrite $MgZnFe_2O_4$ on glass substrate using pulsed- laser ablation method was investigated. The magnetic properties were studied without the addition of any adhesive or fixative. Two samples of thicknesses of (585 nm and 265 nm) ±20 were fabricated. The microwave absorption of the samples was measured at *X*-band within a frequency range of (8-12.5GHz). The frequency absorption and its relationship with the thickness are addressed.

Keywords: Spinel ferrite Pulsed-laser ablation, Vector Network Analyzer.

الخلاصة

تم تحضير الفرايت الهرمي $MgZnFe_2O_4$ باستخدام طريقة صول جل ورسب على الزجاج بطريقة الليزر النبضي. تم دراسة الخواص المغناطيسية من دون إضافة أي مواد لاصق أو مثبت. تم أعداد نماذج بسمكين (٥٨٥ و ٢٦٥)±٢٠ نانومتر بطريقة الليزر النبضي. تم قياس امتصاص أشعة المايكروويف عند X - band مع مدى الترددات (٨-١٢ GHz) للعينتين. تم تناول امتصاص التردد وعلاقته بالسمك.

Introduction

Ferrite materials are important materials in the technological progress. Therefore, the search for what is new to improve their specifications and properties has led to figure out new materials that were not previously known to allow for more applications such as audio converters [1]. The stabilization of the cubic spinel structure was already carried out at ambient settings by spinel-type ferrites (AFe_2O_4) [2]. This specific research has fascinated a substantial concern because of the huge variety and functional efficiency of their chemical and physical properties. The current studies attract a significant interest due to the huge diversity, their chemical and physical properties, functional convenience while comprising oxygen sensing, superparamagnetism, photoelectrical effect, high temperature ceramic, and humidity sensing properties. Ferrite properties are strongly dependent on the chemical structure, cation distribution and sintering temperature, additive quantity of the cations, and methods of urbanization [3]. Nowadays, family of the spinel ferrite are with a chemical formula of (MFe_2O_4), where M indicates the transitional metallic elements, divalent ions, for instance Zn, Co, Mn, Ni, Mg and Cu, , and etc. These are widely used in the mercantile level due to their excellent electrical and magnetic properties [4].

Spinel ferrites were prepared using a dissimilar synthesis technique with main two variant routes for material synthesis [5]. The non-conventional and conventional ceramic wet chemical method that is comprised of a sol-gel technique. This technique is also recognized as chemical solution deposition process, which is extensively used for nanomaterials production whereas initiating from chemical solutions (sol) and also known as precursors [6].

Pulse Laser Ablation (PLA)

Pulsed-laser ablation (PLA) is considered to be an upgraded thermal procedure which is used for compounds and alloys deposition with the help of precise composition of chemicals. A high power pulsed laser (1 J/shot) radiation is discharged through a quartz window on the targeted source material. On the target, the laser power density is increased at the quartz lens. The ablated or evaporated atoms from the surface are gathered on the adjacent surface of the substrate for thin film formation. PLA method benefits from is cell by cell growth direct monitoring reflection high-energy electron diffraction (RHEED)[7].

Microwave Measurements

The relation between the current waveform and voltage waveform is derived from mathematical Telegraphists equation. The distinct reflection coefficient ρ or *Γ* is well defined as the reflected wave ratio to incident wave ratio [8, 9].

$$|\Gamma|^2 = \frac{\text{Reflected power}}{\text{Incident power}} \quad (1)$$

Consider a two-port network in which waves are transmitted in and out of every port generally. In the case of linear device, the output waves are described in relation to input waves. Therefore,

$$b_1 = S_{11}a_1 + S_{12}a_2 \quad (2)$$
$$b_2 = S_{21}a_1 + S_{22}a_2 \quad (3)$$

The measurement of S parameters is possible only in dB decibel. Forms, the conversion of S parameters in percentage (%) form. For this purpose, equation 2 and 3 are used [10]

$$\text{Reflection Coefficient (R\%)} = 10^{\left(S11|_{dB}/10\right)} \quad (4)$$
$$\text{Transmission Coefficient } (T\%) = 10^{\left(S21|_{dB}/10\right)} \quad (5)$$

The substitution of result equation (4) & (5) in (6) equation is carried out by the absorbance (%) [11].

$$A^2 = 1 - R^2 - T^2 \quad (6)$$

Moreover, the reflection loss or attenuation coefficient in dB unit is measured from equation 7 [12].

$$Attenuation\ Coefficient = -20\ Log|S11| \quad (7)$$

Experiment method

The formulation of gel by this technique requires a time for desiccation. This also needs great sintering temperature of 1050°C to attain the phase purification for an extensive time period. The high purity raw materials were selected to evade any effect on the properties of compounds (Mg (NO_3) $2.6H_2O$, Zn (NO_3) $2.6H_2O$, Fe $(NO_3)3.9H_2O$). The ferrite If the samples are prepared by the sol-gel method, the ferrite formula ($Mg_{1-x}Zn_xFe_2O_4$) becomes ($Mg_{0.6}Zn_{0.4}Fe_2O_4$) for when X = 0.4. After the preparation of the samples the product was deposited on the glass after the calculation of the mass needed to be placed in the block of the ferrite in the form of block in pulse laser ablation (PLA) device. Then, it was contained in a flask filled to a certain extent with distilled water and irradiated with laser pluses until it turns into a solution .Then the solution was dropped on the base temperature 85 ^{0}c and then prepare the correct form to obtain the required different thickness without the addition of any adhesive or fixative material and then collected samples and placed inside a cavity for the purpose of preventing moisture and oxidation The magnetic properties were checked by vector network analyzer (VNA) type of Anritsu MS4642A-20GHz.

Results and discussions

Testing Mg-Zn ferrite samples absorbance was performed at the *X*-band range (8-12.5GHz. Figure 1 shows the high absorbance values at 8.21 and 12.37 GHz for thickness 585 nm and both 8.41 and 12.37 GHz for thickness 265 nm.

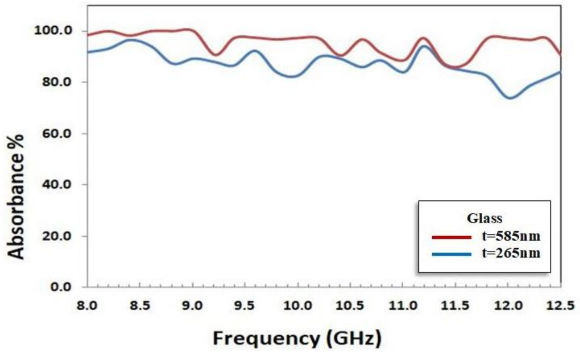

Figure 1: Absorbance curves as a function of frequency at the *X*-band range for $Mg_{0.6}Zn_{0.4}Fe_2O_4$ samples for two thicknesses deferent.

The reduction coefficient with frequency is shown in figure 2. Moreover, the relations between the stability and volatility were noted with the best procedure of consequential outcomes and figure due to the zinc deficiency. There are three peaks of resonance for the samples of $Mg_{0.6}Zn_{0.4}Fe_2O_4$. The formation of the peak was possible when ferrite relative permittivity and relative permeability are identical whereas the finest values of attenuation coefficient were at 585 nm. This was possible because of ferrite completion and augmented density causing the porosity reduction. Thus, the maximum attenuation coefficient values at 585nm are (-31.17,-33.08,-34.25) dB having frequencies (8.61, 10.01, 10.60) GHz, respectively.

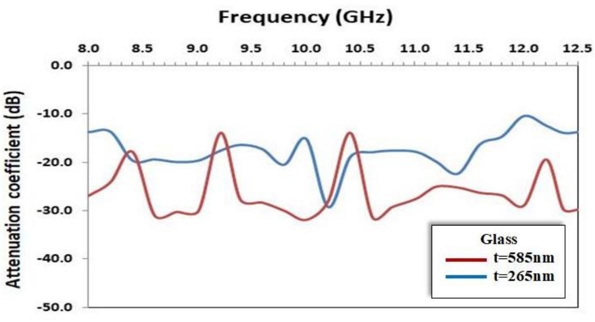

Figure 2: Attenuation coefficient as a function of frequency at the *X*-band range for $Mg_{0.6}Zn_{0.4}Fe_2O_4$ samples for two thicknesses deferent.

Figure 3 shows reflection coefficient near zero except for some regions due to heterogeneity of the thin film and appearance of one resonance peak in the resulting figure between (8.20-9.61) GHz for (585) nm and between (8.00-8.81) GHz for (265) nm are considered abnormal. The reflection coefficient top values can be observed at 585nm as a result of an upsurge in density that lessens the porosity and ferrite completion in class as well. The uppermost reflection coefficient values for 585nm were (-1.035, -1.59) dB at (9.81 & 8.82) frequencies respectively.

The overlapping of the transmission coefficient value at two thicknesses 265nm and 585nm is shown in figure 4 that authorizes the ferrite formation amongst the two thicknesses.

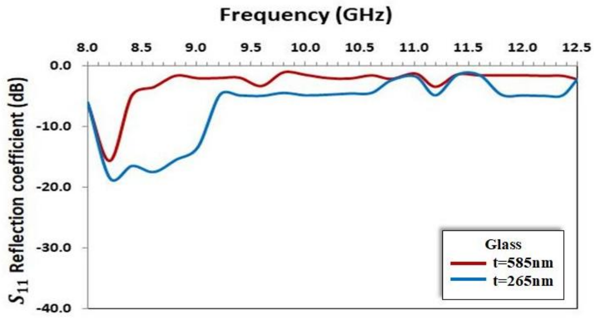

Figure 3: The reflection coefficient (S_{11}) as a function of frequency at the *X*-band range for $Mg_{0.6}Zn_{0.4}Fe_2O_4$ samples for two thicknesses deferent.

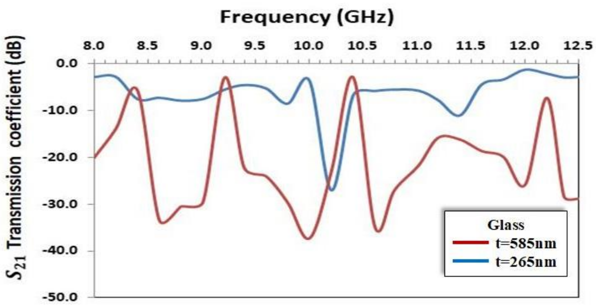

Figure 4: The transmission coefficient (S_{21}) as a function of frequency at the *X*-band range for $Mg_{0.6}Zn_{0.4}Fe_2O_4$ samples for two thicknesses deferent.

There is one resonance peak (-22.07dB) for the $Mg_{0.6}Zn_{0.4}Fe_2O_4$ sample sintered at 1050°C for two thicknesses 585 nm and 265 nm. The formation of peak is possible with equivalent relative ferrite's permittivity and permeability. The best attenuation coefficient values can be seen for 585nm caused by ferrite completion in this class and porosity reduction by amplified density. The greatest attenuation coefficient's values at 585nm are (-22.04, -28.37) dB at (11.40, 10.21GHz) frequencies respectively.

The outcomes of entire Mg-Zn ferrite formulas, as well as their deposition on Glass for two deferent thicknesses, are listed in the table 1. The reason of bandwidth is matching at most frequencies, causing the peaks to unite and producing a single resonance peak. The reason in this is the value of thickness 585 nm (the proportion of zinc) appropriate to make this matching.

Table 1: The absorbance result for the $Mg_{0.6}Zn_{0.4}Fe_2O_4$ samples for two thicknesses deferent.

Thickness in (nm) ±20	No. of Resonance peaks	good bandwidth length in (GHz)	frequencies range in (GHz)		Absorbance range %	
585	3	0.90	9.60	8.81	98.45	96.14
	3	1.22	11.20	12.01	98.37	97.32
265	3	1.15	8.40	9.60	96.94	92.65
	3	1.10	10.21	11.20	89.75	94.21

By comparing the results of the samples for two thicknesses, it is noticed that the results of 585 nm are better than those of 265 nm, due to the high conductivity of 265 nm that is caused the reflection of incoming waves which reduces the absorbance.

Conclusions

Preparation of samples in a sol-gel method gives rise to synthesis of ferrite nanostructures. The absorbance of increases with increased thicknesses of the samples because the attenuation and the absorbance cause an interaction of spin-spin. The use of the method of PLA for the ferrite on the glass gives steadier and stability than other methods of precipitation. The thickness of the deposited ferrite has a direct relationship where the higher the thickness the higher the absorption and the lower the reflection and transmission of the samples.

References

[1] S. Vijayanand, "Synthesis and characterization of spine type magnetic and non-magnetic oxide nanomaterials," 2010.

[2] Z. Wang, D. Schiferl, Y. Zhao, and H. S. C. O'Neill, "High pressure Raman spectroscopy of spinel-type ferrite ZnFe2O4," *Journal of Physics and Chemistry of Solids,* vol. 64, pp. 2517-2523, 2003.

[3] M. Jamil, J. Ahmad, S. Bukhari, T. Sultan, M. Akhter, H. Ahmad, *et al.*, "Effect on structural and optical properties of Zn-substituted cobalt ferrite CoFe 2 O 4," *Journal of Ovonic Research,* vol. 13, pp. 45-53, 2017.

[4] N. Sezgin, M. Sahin, A. Yalcin, and Y. Koseoglu, "Synthesis, characterization and, the heavy metal removal efficiency of MFe2O4 (M= Ni, Cu) nanoparticles," *Ekoloji,* vol. 22, pp. 89-96, 2013.

[5] N. Sanpo, "Fabrication and Characterisation of Cobalt Ferrite Nanoparticles and SPPS-Deposited Cobalt Ferrite Splats Prepared by Sol-Gel Methods," 2014.

[6] A. Sutka and G. Mezinskis, "Sol-gel auto-combustion synthesis of spinel-type ferrite nanomaterials," *Frontiers of Materials Science,* vol. 6, pp. 128-141, 2012.

[7] P. Whiteside, J. Chininis, and H. Hunt, "Techniques and challenges for characterizing metal thin films with applications in photonics," *Coatings,* vol. 6, p. 35, 2016.

[8] A. Basu, *An introduction to microwave measurements*: CRC Press, 2014.

[9] R. Collier and A. Skinner, "Microwave Measurements 3rd edition. London: Institution of Engineering and Technology," 2007.

[10] Z. Popovic and E. F. Kuester, "Principles of RF and Microwave Measurements," *University of Colorado, Electromagnetics Laboratory Department of Electrical and Computer Engineering Campus Box,* vol. 425, pp. 80309-0425, 2005.

[11] D. B. Davidson, *Computational electromagnetics for RF and microwave engineering*: Cambridge University Press, 2010.

[12] A. L. Lance, *Introduction to microwave theory and measurements*: Glencoe/McGraw-Hill School Pub Co, 1964.